



UNIVERSITY OF LEEDS

This is a repository copy of *Evaluation of Mechanical and Thermal Properties of Carrageenan/Hydroxypropyl Methyl Cellulose Hard Capsule*.

White Rose Research Online URL for this paper:

<https://eprints.whiterose.ac.uk/189778/>

Version: Accepted Version

Article:

Ramli, NA, Adam, F, Mohd Amin, KN et al. (2 more authors) (2023) Evaluation of Mechanical and Thermal Properties of Carrageenan/Hydroxypropyl Methyl Cellulose Hard Capsule. *The Canadian Journal of Chemical Engineering*, 101 (3). pp. 1219-1234. ISSN 0008-4034

<https://doi.org/10.1002/cjce.24595>

This article is protected by copyright. All rights reserved. This is the peer reviewed version of the following article: Ramli, N.A., Adam, F., Mohd Amin, K.N., M. Nor, A. and Ries, M.E. (2022), Evaluation of Mechanical and Thermal Properties of Carrageenan/Hydroxypropyl Methyl Cellulose Hard Capsule. *Can J Chem Eng*. Accepted Author Manuscript which has been published in final form at <https://doi.org/10.1002/cjce.24595>. This article may be used for non-commercial purposes in accordance with Wiley Terms and Conditions for Use of Self-Archived Versions. This article may not be enhanced, enriched or otherwise transformed into a derivative work, without express permission from Wiley or by statutory rights under applicable legislation. Copyright notices must not be removed, obscured or modified. The article must be linked to Wiley's version of record on Wiley Online Library and any embedding, framing or otherwise making available the article or pages thereof by third parties from platforms, services and websites other than Wiley Online Library must be prohibited.

Items deposited in White Rose Research Online are protected by copyright, with all rights reserved unless indicated otherwise. They may be downloaded and/or printed for private study, or other acts as permitted by national copyright laws. The publisher or other rights holders may allow further reproduction and re-use of the full text version. This is indicated by the licence information on the White Rose Research Online record for the item.

Takedown

If you consider content in White Rose Research Online to be in breach of UK law, please notify us by emailing eprints@whiterose.ac.uk including the URL of the record and the reason for the withdrawal request.



eprints@whiterose.ac.uk
<https://eprints.whiterose.ac.uk/>

Ries Michael E. (Orcid ID: 0000-0002-8050-3200)

Evaluation of Mechanical and Thermal Properties of Carrageenan/Hydroxypropyl Methyl Cellulose Hard Capsule

Nur Amalina Ramli¹, Fatmawati Adam^{1,2}, Khairatun Najwa Mohd Amin¹, Adibi M. Nor³, Michael E. Ries⁴

¹*Faculty of Chemical and Process Engineering Technology, Universiti Malaysia Pahang, Kuantan, Pahang, Malaysia*

²*Centre for Research in Advanced Fluid and Processes, Universiti Malaysia Pahang, Kuantan, Pahang, Malaysia*

³*Institute for Advanced Studies, University of Malaya, Kuala Lumpur, Malaysia*

⁴*School of Physics & Astronomy, University of Leeds, Leeds, United Kingdom*

Correspondence

Fatmawati Adam, Faculty of Chemical and Process Engineering Technology, Universiti Malaysia Pahang, 26300 Kuantan, Pahang, Malaysia

Email: fatmawati@ump.edu.my

Abstract

The inherent source of gelatin used for commercial hard capsules causes a surging demand on vegetarian capsules. In this work, carrageenan is utilized in preparing hard capsules to meet consumer preferences. Hydroxypropyl methylcellulose (HPMC) was incorporated as a reinforcing agent to improve the low mechanical properties of hard capsules made of carrageenan. HPMC concentration was manipulated from 0.2 w/v% to 1.0 w/v% in the carrageenan matrix. Increasing concentration of HPMC exerts significant effects on the tensile strength and elongation at break, with an improvement of 59.1% and 46.9%, respectively, at the optimized HPMC concentration of 0.8 w/v%. The loop strength of the capsule is also increased by 56.4% with decreasing moisture content. A downfield movement around 3.20 ppm of the carrageenan proton to 3.33 ppm in ¹H-NMR spectrum suggests the formation of intermolecular hydrogen bonding between carrageenan and HPMC, which correlates to the results of FTIR and zeta potential. The glass transition of the film is increased from 37.8°C to 65.3°C, showing an upgrade in thermal stability. The film possesses a major mass loss with an activation energy of 64.7 kJ/mol with an increment of 43.4% compared to the control carrageenan. These findings

This article has been accepted for publication and undergone full peer review but has not been through the copyediting, typesetting, pagination and proofreading process which may lead to differences between this version and the [Version of Record](#). Please cite this article as doi: [10.1002/cjce.24595](https://doi.org/10.1002/cjce.24595)

This article is protected by copyright. All rights reserved.

support the conclusion that HPMC enhanced the mechanical properties and thermal stability of the carrageenan film, and the comprehensive analysis of the molecular interaction and decomposition kinetics subsequently may expand the application fields of the carrageenan-HPMC hard capsule as an alternative to gelatin in the future.

KEYWORDS

activation energy, carrageenan, hydroxypropylmethyl cellulose, mechanical strength, thermal stability.

1 INTRODUCTION

Hard capsules are predominantly employed dosage form for oral administration of active ingredients due to their simplicity and ease of manufacture.^[1] At present, gelatin is the most widely applied material and remains appealing to hard capsule manufacturers because it is soluble in biological fluids at body temperature, and forms a strong, flexible and homogeneous film.^[2] Despite these advantages, its inherent source from animals has given rise to a huge concern towards consumers' preference based on the vegetarian dietary requirement. Gelatin is commonly extracted from mammals, mainly porcine and bovine.^[3] Considering the awareness of this issue, great attempts are being conducted to search for an alternative capsule material, preferably of plant origin, and able to present comparable properties and performance to gelatin. Hydroxypropyl methyl cellulose (HPMC) and pullulan hard capsules have been successfully introduced in the current market.^[4] The development of plant-based hard capsule is progressing with the exploration of new plant materials from cellulose,^[4,5] starches,^[6,7] gellan and xanthan gums.^[8] In this work, carrageenan-based hard capsule with HPMC incorporation is developed to replace gelatin.

Carrageenan is a sulphated linear polysaccharide with three different isomers.^[9,10] The isomers exhibit different chemical structures and gelation properties according to their ester sulphate content; kappa (κ) (20%), iota (ι) (33%) and lambda (λ) (41%).^[11,12] Studies which relate to film-forming application is majority subjected to κ -carrageenan, due to its ability to form a rigid film with the highest mechanical strength compared to ι - and λ -carrageenan.^[12-14] Carrageenan offers value-added properties in food and pharmaceutical products as a thickener, stabilizer, coagulant, and emulsifier which assured its surging market demand.^[15,16] Considering these key attributes, carrageenan can be a promising option as an alternative to gelatin.

In contempt of that, carrageenan-based hard capsule, which is from natural biodegradable polymer exhibits low mechanical strength which restricts its applicability and

Accepted Article

feasibility in production.^[14,17] A multitude of chemical modifications have been studied to modulate the mechanical properties of carrageenan hard capsules. The incorporation of 2.0 wt.% carboxymethyl cellulose (CMC) substantially increased the viscosity of carrageenan composite up to 50% and the tensile strength of the film up to 37%.^[18] The inclusion of 1.6 wt.% cellulose nanocrystals (CNC) resulted in an increment by 58% of the tensile strength.^[5] The effect of physical crosslinking with the inclusion of 3 wt.% isovanillin in the composite was also proven to improve the tensile strength up to 49%.^[19] Blending with Arabic gum enhanced the capsule strength at a mass ratio of 67 wt.% carrageenan.^[13] A thorough study on the mixing time in preparing hard capsule was conducted to optimize its mechanical properties.^[17] Blends of higher concentrations of carrageenan with Arabic gum and polyethylene glycol induced higher activation energy (E_a) on the film decomposition.^[20] The most important characteristic of a film-based product is its ability to withstand mechanical damage and exhibit an appropriate level of flexibility for ease of handling and processing.^[21]

HPMC, an excipient functions as a reinforcing agent, is introduced in the formulation to deal with the brittleness of carrageenan hard capsules. HPMC is a recurrent hydrophilic polymer of choice over other cellulose derivatives due to its excellent thickening, film-forming, swelling, and miscibility.^[16,22] The capsules made up of HPMC are less brittle and can exhibit higher tensile strength even with lower moisture content compared to gelatin.^[22] HPMC can form a hydrogel at high temperature as opposed to the gelation upon-cooling property of carrageenan.^[23] The gelation capacity of HPMC decreases at low temperatures. This is one of the issues to prepare HPMC hard capsules, where the adjustment of the pin temperature is needed. The pins must be maintained at higher temperatures to prevent the liquefaction of the films formed on the pins.^[2] When HPMC is mixed with carrageenan, metal pins can be dipped in a warm composite solution at room temperature, which is similar to those used for gelatin. Therefore, no special procedures are needed and the existing manufacturing apparatus for immersion and moulding of traditional gelatin capsules can be used without modification.

Even though there are numerous studies available on plant-based hard capsules, it is still important to develop a composite matrix with improved properties to be comparable to gelatin.^[24,25] Moreover, there are limited reports that exist on the use of HPMC as a reinforcing agent in preparing carrageenan hard capsules.^[16] There is further scope to provide an understanding on the molecular interaction mechanism and E_a of decomposition related to the mechanical and thermal properties of the hard capsule. The stability of particles in the carrageenan matrix through zeta potential analysis is also a significant study to prevent the formation of aggregation. This work aims to evaluate the mechanical properties of Carra-HPMC

composite film and to study its thermal properties through the E_a of decomposition. Blend of carrageenan and HPMC to form composite for hard capsule through hydrogen bonding networking is hypothesized to increase the mechanical and thermal properties by formation of intermolecular interaction.

2 MATERIALS AND METHODS

2.1 Materials

Refined carrageenan was purchased from CV Simpul Agro Globalindo, Indonesia (molecular weight ranges from 930 to 1010 g/mol with 31.5% carbon, 5.97% hydrogen, 0% nitrogen, and 6.28% sulphur.^[19] Hydroxypropylmethyl cellulose (average molecular weight of 86 kDa), 4-methoxybenzyl alcohol (98%) (anise), and calcium alginic acid (alg) were obtained from Sigma-Aldrich (USA). Polyethylene glycol (PEG) as a plasticizer was purchased from Merck (Germany). All chemicals used are of analytical grade.

2.2 Preparation of film and hard capsule

Table 1 summarizes the formulation which was used to prepare Carra-HPMC composite film. The solution of refined carrageenan (3.0 g) mixed with 0.2 w/v% to 1.0 w/v% of HPMC was prepared in 150 mL of deionized water at 60°C. Formulation without the addition of HPMC was used as a control. The same amount of anise (0.7 v/v%), polyethylene glycol (0.3 v/v%), and calcium alginic acid (0.07 w/v%) was then added to each sample as a crosslinker, plasticizer, and toughening agent, respectively. After 3 hours of mixing, approximately 20 mL of the solution was poured into a stainless-steel tray with a diameter of 20 cm. The sample was left overnight at room temperature to form a film. Meanwhile, the other portion of the solution was dipped using stainless-steel mould capsule pins size “1” to prepare hard capsules. The dried resulting film and hard capsules were then employed for characterization and analysis.

2.3 Zeta potential measurement

Zeta potential of the sample was measured to evaluate the stability of the composite to reduce the tendency of the materials to flocculate and prevent agglomeration after film drying. The zeta potential of Carra-HPMC composite was measured using a DelsaMax Pro zeta potential analyzer (Beckman Coulter, UK), utilizing the phase analysis light scattering (PALS) technique.^[26] The sample was diluted with deionized water to a final concentration of 0.1 v/v%. The Bi-PALS software provided an average of electrophoretic mobility and measured the zeta-potential using the Smoluchowski model.^[27]

2.4 ¹H-NMR spectroscopy analysis

NMR analysis was conducted to acquire molecular-level insight through the changes of the ¹H spectrum of Carra-HPMC composite to identify preferential intermolecular interactions that occur. The 500 MHz of ¹H NMR spectra were recorded using an NMR spectrometer (Bruker Ultra Shield Plus, Germany) which operated at room temperature. Samples were prepared in DMSO-d₆ and tetramethylsilane (TMS) as the internal standard.^[28] The chemical shifts were measured with respect to the remaining proton resonance of DMSO-d₆ (2.50 ppm).^[29]

2.5 FTIR spectroscopy analysis

FTIR spectra of the film were measured by ATR-FTIR spectrometer (Perkin Elmer, USA) to recognize any potential shifting of the hydrogen bonding structure in the composite. A total of 16 scans were acquired at 0.15 s/scan and with a spectral resolution of 8 cm⁻¹ within the range of 400 to 4000 cm⁻¹. The spectra were analyzed using OMNIC software.^[19]

2.6 Viscosity measurement

The viscosity of carrageenan composite was measured using a rotational rheometer (Rheo3000, USA) equipped with LCT 25 4000010 geometry. The viscosity will reflect to the film tensile strength and the capsule loop strength. Approximately 15 mL of the composite solution was filled in the measuring block. The measurement was programmed at a speed of 300 revolutions per minute, with 100 MPoints at a pre-heated temperature of 40°C.^[18]

2.7 Mechanical properties analysis

The mechanical analysis was conducted to examine the deformation of the prepared film and hard capsule to an applied load or force. The tensile strength and elongation at break of 2 cm × 6 cm Carra-HPMC film strips were measured using a texture analyzer (CT3, USA) equipped with a 5 kN load cell. The trigger force was applied at a crosshead speed of 30 mm/min to a maximum distance of 15 mm.^[5] A hard capsule loop test was also conducted using the same texture analyzer (CT3, USA). The target value of 5.0 mm and the speed of 0.50 mm/s were predetermined.^[13] The maximum force (N) used to tear the hard capsule before rupture was recorded as an indication of the loop strength of the hard capsules.

2.8 Moisture content analysis

The moisture content of a sample can affect its mechanical properties, as well as its thermal stability. Therefore, the moisture content of the film was determined by using a moisture analyzer (MS70, A&D, Japan). The moisture content was calculated in mass on completion of

the heating regime compared to the initial mass of 0.1 g of the sample.^[30] The measurement would stop once the sample attained a constant value of moisture content.

2.9 Disintegration test

Following United States Pharmacopeia (USP), a disintegration test was performed using a disintegration tester (Distek 3100, Germany), in which capsules were placed in the tubes and then immersed in 600 mL of distilled water at $37 \pm 2^\circ\text{C}$.^[19] For ease of observation, the capsules were filled with lactose as a placebo. The disintegration time of the capsules was measured as the time (minutes) required for the lactose placebo to initially diffuse from the capsules into the medium.

2.10 Morphological analysis

The morphology of Carra-HPMC film surface was observed using the scanning electron microscope (S26000-N Hitachi, Japan). The sample was sputter-coated with a platinum film to prevent any charging up to the surface by the electron beam.^[13] The film was observed under $3000\times$ magnification to characterize the surface morphology and presence of agglomeration on the sample surface.

2.11 Thermal stability analysis

The thermograms of the films were recorded by differential scanning calorimeter (DSC) (Polyma214, Germany) to determine the glass transition, melting and crystallization temperatures for the thermal stability of the composite film. Approximately 3 mg of the sample was heated at $10^\circ\text{C}/\text{min}$ from 30°C to 400°C in a nitrogen atmosphere.^[13] Thermographic profiles of carrageenan films were analyzed using a thermogravimetric analyzer (TGA) (STA7200 Hitachi, Japan). Approximately 3 mg of the film was heated in the airflow from 30°C to 700°C at $10^\circ\text{C}/\text{min}$.^[16] Mass loss and differential thermal analysis profiles were also reported.

2.12 Kinetic analysis by Broido's model

The kinetic analysis was conducted to calculate the E_a on the maximum degradation temperature of the sample, following the Arrhenius kinetic theory based on the results of DSC and TGA. E_a is the minimum energy required to break the bond between molecules in the structure of the material during thermal degradation.^[20] At first, the degree of conversion was calculated using Equation (1) as follows:

$$y = \frac{w_t - w_\infty}{w_0 - w_\infty} \quad (1)$$

where y is the degree of conversion, w_t is the weight at any time in gram, w_0 is the initial weight, and w_∞ is the weight of residue. Based on the degree of conversion, a graph was drawn by plotting $\ln [\ln (1/y)]$ vs $1000/T$, where the value of E_a was provided from the slope of the graph^[31,32] as in Equation (2):

$$\ln \left[\ln \left(\frac{1}{y} \right) \right] = - \left(\frac{E_a}{RT} \right) + \ln A \quad (2)$$

where R is the universal gas constant ($R = 8.314 \text{ J}\cdot\text{mol}^{-1}\cdot\text{K}^{-1}$), E_a is the activation energy (kJ/mol), T is the temperature recorded in thermogram (K), and A is the pre-exponential factor (min^{-1}). The entropy of activation (ΔS), enthalpy of activation (ΔH), and Gibbs free energy change (ΔG) were also calculated based on the activation energy.

2.13 Statistical analysis

All measurements were presented as the mean \pm standard deviation from at least three independent experiments. The one-way analysis of variance (ANOVA) was performed to calculate the confidence level of p -value, where $p < 0.05$ was regarded as statistically significant. The testing null analysis (H_0) and alternative analysis (H_i) were assigned for viscosity, tensile strength, elongation at break, capsule loop strength, moisture content, and disintegration time.

3 RESULTS AND DISCUSSION

3.1 Zeta potential of biocomposite

The zeta potential values of carrageenan, HPMC, and other materials in the composite are all in negative values (Figure 1A). The zeta potential of carrageenan has the highest negative value which is -54.0 mV . It is similar to the result found by Ellis et al.^[33] and it reflects the negatively charged ester sulphate groups of carrageenan, while HPMC is -3.94 mV which is slightly negative as reported by Nemazifard et al.^[34] The reduction in net negative charges of carrageenan composite added with the increasing amount of HPMC can be linked to the interaction between both materials (Figure 1B). It can be speculated that the helix structure of carrageenan is surrounded by HPMC and prompts the reduction of zeta potential of the composite. Nonetheless, it is considered to have a high value of zeta potential $\geq 30 \text{ mV}$ indicating a physically stable dispersion due to the predominance of electrostatic repulsion over Van der Waals forces.^[30,35]

3.2 ¹H-NMR spectroscopy of biocomposite

Molecular structure of carrageenan can be divided into two units as in Figure 2A, namely G-unit which refers to alternating 3-linked β -D-galactopyranose, and DA-units which refers to 4-linked 3,6-anhydro- α -D-galactopyranose.^[36] (G-1 (1H; 5.01 ppm), G-2 (O-2H; 3.27 ppm), G-3 (2H; 3.87 ppm), G-4 (1H; 4.96 ppm), and G-5,6 (O-2H; 3.51 ppm) are the six sites of chemical shift at G-unit. Meanwhile, there are also six chemical points for the DA-unit: DA-1 (1H; 4.97 ppm), DA-2 (O-2H; 4.16 pm), DA-3 (O-1H; 4.34 ppm), DA-4 (O-1H; 4.91 ppm), DA-5 (1H; 4.69 ppm), and DA-6 (2H; 4.16 ppm). These spectral peaks are consistent with those discovered by Abu Bakar^[37] and Voron'ko^[38], but with minor shifts that could be attributed to differences in sample preparation.

In the raw HPMC spectrum, the polymer repeating unit protons exhibited the resolved signals at 2.41-3.64 ppm (H-1-8, H-10) (Figure 2B). These multiple peaks assign to the methyl protons adjacent to the oxygen moieties of ether linkages (O-CH₃), inner methylene (O-CH₂) and methine protons (-CH-O), and HPMC backbones of anhydroglucose unit.^[28] Another single signal that appeared at 1.02 ppm (H-9) is associated with the methyl protons in the hydroxypropyl moieties of HPMC (3H, CH-CH₃). Signal assignment observed of HPMC appears at lower chemical shift but corresponds to the one reported by Lu et al.^[39] (2.75-4.75 and 1.05 ppm) and Amin et al.^[40] (2.89-5.10 and 1.13 ppm). Different sources of sample and different sample treatment prior to analysis might be the reasons of this variation.

Hydrogen bond formation causes shifts to a higher frequency (higher ppm) owing to deshielding and the electronegativity increases. The peak that corresponds to the proton at 3-linked β -D-galactopyranose (G)-2 (O-2H) of carrageenan spectrum around 3.2 ppm^[36] has a slight downfield movement to 3.33 after incorporation of HPMC, which is thought to be caused by the formation of intermolecular hydrogen bonds between carrageenan and the HPMC molecule. This indicates the molecular distribution of HPMC surrounds the helix structure of carrageenan as mentioned in zeta potential analysis. There are also additional minor peaks detected at around 3.35-3.38 contributed by the interaction between these two materials (Figure 2C). A change in the integration values of the area between 2.35-2.99 is observed in Table 2, which shows an increasing number of protons detected bounded to Carra-HPMC composite compared to the raw materials. Peaks at this range depict upfield chemical shifts to lower frequency after being introduced in carrageenan matrix attributed to the hydrophobic interaction between highly methylated glucose zones of HPMC.^[41] This type of interaction occurs during the gelation of HPMC which increases the viscosity of the composite for reinforcement. Meanwhile, chemical shifts of HPMC at 1.0-1.3 ppm deshielded to a higher frequency, which

prescribed that hydrogen bond interaction with carrageenan could also occur at H9 (methyl protons of the hydroxypropyl group).

Figure 3 depicts a film-forming mechanism based on the proposed hydrogen bonding interaction between carrageenan and HPMC corresponding to the NMR results. The molecules of carrageenan and HPMC are initially dispersed randomly in the solution. Carrageenan interacted with HPMC via intermolecular hydrogen bonding, and both molecules' three-dimensional network structures are entangled and formed inter-phases. Cross-linking and gelation are also caused by the intermolecular interactions of the hydrophobic groups of the HPMC chains. The formation of carrageenan-HPMC composite provides a synergistic effect on enhancing the mechanical properties, which are attributed to interpenetration between the two polysaccharides. In verification of the hypothesis, the mechanical properties of Carra-HPMC composite film and hard capsule are examined and its subsequent improvement on thermal properties is investigated.

3.3 FTIR spectroscopy of film

Figure 4A depicts the spectra of carrageenan and HPMC as the raw materials together with the spectrum of Carra-HPMC composite film. Carrageenan prompts its characteristic peaks at 1223 cm^{-1} and at 1034 cm^{-1} which indicate the -SO sulphate esters and the glycosidic linkage (-CO) of carrageenan, respectively. The characteristic peak of 3,6-anhydro-D-galactose appears at 921 cm^{-1} while the peak at 841 cm^{-1} is attributed to C-O-SO₄ on D-galactose-4-sulphate. The spectrum of carrageenan is comparable with the findings presented in the literature.^[16,19,42] The expanded band centres around 3443 cm^{-1} and the peak at 2900 cm^{-1} refer to the -OH and -CH stretching vibrations, respectively, which are also detected in the spectra of HPMC and Carra-HPMC film.

In the spectrum of HPMC, the band at 1638 cm^{-1} is associated with the C=O group while the absorption peak at 1453 cm^{-1} refers to the -CH scissoring. These correspond to the results found by Liu et al.^[23] and Bodini et al.^[43] for HPMC-based films. Meanwhile, the characteristic peaks of cellulose C-O-C in HPMC are detected around the same region as reported by Pacheco-Quito et al.^[44] and Suksaeree et al.,^[45] which are at 1060 cm^{-1} and 958 cm^{-1} .

Carra-HPMC film presents similar spectra with identical functional groups of raw carrageenan and HPMC. An increase in the peak intensity of the hydroxyl band of Carra-HPMC film is owing to the increase in the amount of -OH bond, implying hydrogen bonding formed between carrageenan and HPMC. The addition of HPMC also altered the -SO peak of carrageenan at 1223 cm^{-1} , which for the composite film was not as intense as that for

carrageenan film. This indicates the occurrence of intermolecular interaction between carrageenan sulphate ester groups and hydroxyl groups of HPMC, forming a more compact and rigid structure of composite film.

FTIR spectra of all prepared films with different HPMC concentrations are reported in Figure 4B for a thorough understanding of the created hydrogen bonding between the molecules. It is expected that this interaction would exist between the hydroxyl groups of carrageenan and HPMC.^[16] The regions of hydroxyl groups situated at 3700-3200 cm^{-1} are focused on determining the shifted peak and its intensity. As the HPMC concentration increases from 0.2 to 0.8 w/v%, the hydroxyl band moves from 3394 cm^{-1} to a lower wavenumber of 3382 cm^{-1} with increasing intensity, suggesting that a greater intermolecular hydrogen bond was formed between the materials.^[46] This interaction corresponds to the NMR results as discussed in the previous section. The improved hydrogen bonding interaction will lead to an increment in film strength.^[17]

3.4 Viscosity of biocomposite and mechanical properties of film and hard capsule

The presence of HPMC causes the viscosity to increase significantly ($p < 0.05$) from 172.1 mPa·s to its highest point achieved at 0.8 w/v% with 616.5 mPa·s (Figure 5A). The higher concentration of HPMC in the formulation retards the flow of the composite, resulting in higher viscosity.^[47,48] The direct correlation between viscosity and the mechanical strength is displayed in the same figure where the results depict a similar profile with the same optimum point at Carra-HPMC0.8. The higher viscosity of composite leads to a higher tensile strength.^[49] It is notable that Carra-HPMC0.8 achieved the highest strength of 51.2 MPa. Great difference ($p < 0.05$) in tensile strength related to the incorporation of HPMC is observed when the strength was optimized up to 59.1%.

Carra-HPMC0.8 film could endure higher applied pressure up to 47.3% and displays a higher resistance to mechanical stress compared to the control film with 14.5% ($p < 0.05$) (Figure 5B). The high viscosity of HPMC gives rise to the breaking point and exhibits flexibility of the film, thereby implies a greater resistance to break under tension. More effective resistance against external load could be due to the compactness of the blending polymer, where HPMC fills the voids in restructuring the carrageenan film.^[50] The capsule loop strength is also significantly enhanced by 56.4% ($p < 0.05$) to a maximum of 37.4 N at the same concentration before falling to 27.8 N at 1.0 w/v%. The viscosifying effect of HPMC enforces the physical structure of the film and serving as a reinforcing agent. In capsule manufacturing, forming

harder and stronger capsules translates into lesser defects and lower rejection rates during capsule filling.

Despite that, a higher concentration of Carra-HPMC1.0 expecting of agglomeration and has disturbed the intermolecular interaction between carrageenan and HPMC, thus reduced the viscosity of the composite.^[51] At this point, the increase of HPMC concentration is most likely not resulted in higher tensile strength because the maximum ability of the film to restrain the applied load is reached. Instead, the tensile strength is decreased abruptly. It has overridden the reinforcement effect on the carrageenan film. Moreover, there might be an insufficient amount of plasticizer in the matrix that inhibits the flexibility and continuity of the matrix chain.^[52]

In comparison with commercial hard capsule, there is still a gap on the properties between Carra-HPMC and gelatin hard capsule as tabulated in Table 3. The ideal viscosity of gelatin solution has been reported to range between 750 to 1000 mPa·s.^[53,54] The viscosity provides an insight into the behaviour and intermolecular interaction between the composite chains and gives an indication of its performance. With higher viscosity, gelatin hard capsule presents a higher loop strength and melting temperature compared to Carra-HPMC. Meanwhile, these two types of hard capsules have the similar moisture content and disintegration time.

3.5 Moisture content of film and disintegration time of hard capsule

Control film without incorporation of HPMC has the highest moisture content with 23.2% (Table 4). This is due to the fact that carrageenan is composed of sulphate groups which impart higher hydrophilicity.^[57] Increasing concentration of HPMC greatly decreases ($p < 0.05$) the affinity of film to adsorb more water. When water adsorption of the films is low, it enhances the tensile strength of the film and reduces its brittleness.^[58] The moisture content of Carra-HPMC0.8 is 14.6% and it displays the optimum mechanical strength among others. This value is comparable to that of commercial gelatin capsules (13%) even it is greater than commercial HPMC capsules (4.5%).^[56] Carra-HPMC1.0 shows the lowest moisture content; however, its decreased mechanical properties give drawbacks in forming capsules.

The control hard capsule disintegrates after 10.6 min while increased disintegration time is reported as the concentration of HPMC is increased. High molecular weight and viscosity of HPMC together with the gel promoter of carrageenan cause a delay in the initial burst of the capsule in aqueous medium. Fu et al.^[59] emphasized that higher viscosity and molecular weight of the polymer tend to dissolve slower because of greater entanglement and higher gel viscosity.

This explains the increasing disintegration time of Carra-HPMC capsules with increasing concentration of HPMC.

Carra-HPMC0.8, which is the best concentration of HPMC based on mechanical properties, takes 18.7 min to dissolve, exhibiting a longer disintegration time than the control capsule, with $p < 0.05$ indicating a significant difference between capsules of all formulations. Carrageenan hard capsule crosslinked with maltodextrin was reported to disintegrate in 18 minutes, while gelatin and HPMC capsules were within 15 and 30 minutes, respectively.^[9,60] The time frame of 30 minutes satisfying the USP criteria for dietary supplement formulations.^[2,60] Delayed *in vivo* disintegration of HPMC capsules, however, does not give a negative effect *in vivo*.^[2] Thus, HPMC capsules can be comparable to gelatin capsules.

3.6 Physical appearance and surface morphology of film

Visually, the transparency and gloss of composite films and hard capsules are retained until the addition of 0.8 w/v% of HPMC (Figure 6). The uniform matrix depicts the compatibility between the materials due to uniform mixing.^[19] This shows good miscibility between carrageenan and HPMC. Excess addition of HPMC (1.0 w/v%) in the formulation results in a heterogenous film with increased thickness and less opacity. SEM image of Carra-HPMC1.0 shows that macromolecules are visible at the film surface, possibly due to the deformation forces acting during the polymer chain aggregation during solvent evaporation.^[61] This result explains the translucent film exhibited at this concentration. Non-uniformity of polymer matrix due to excess inclusion of HPMC intensifies the film brittleness, thereby leading to poor mechanical properties. The non-uniform dispersion may also be attributed to the poor mixing because of the highly viscous effect of HPMC.

3.7 Thermal analysis of film

The thermal properties attributed to the composite materials are scrutinized since they could affect their applicability to be marketed in the form of hard capsules. A significant drawback of biopolymers is their poor thermal stability compared to synthetic polymers. Carra-HPMC0.8 film presents optimum mechanical strength in terms of tensile strength, elongation at break, and capsule loop strength. Therefore, a thermal stability study was conducted using DSC and TGA for Carra-HPMC at this concentration.

3.7.1 DSC analysis

The heating profiles for Carra-HPMC at all concentrations are illustrated in Figure 7 with pure carrageenan and HPMC. Glass transition temperature (T_g) of every film is investigated since it

Accepted Article

is a rescindable transition in amorphous or in some cases semi-crystalline constituents from a stiff glassy state to a rubbery state.^[62] The film changes from elastic to brittle due to changes in chain mobility. In Table 5, the T_g of carrageenan film is 40.3°C. This value is lower compared to the previously reported T_g of carrageenan which ranging from 50°C to 70°C.^[63,64] Probably, the differences in preparation method and heating rate may affect the T_g values. The control film of carrageenan possesses a lower T_g (37.8°C) because of the presence of plasticizers which leads to the formation of hydrogen bonds with polymeric chains and increases the free volume in the structure, thus facilitates mobility of carrageenan chains at lower temperatures.^[65] Meanwhile, T_g of HPMC film is recorded at 143.4°C. The previously reported T_g is slightly higher in the range of 150°C to 180°C.^[21,47] Another apparent endothermic peak is observed at 358.8°C due to HPMC thermal decomposition.

Notably, T_g of the control film is shifted by 42.1% from 37.8°C to 65.3°C after the inclusion of HPMC, indicating a structure modification in the matrix (Table 5). It could be ascribed to the mobility restriction imposed by HPMC added in the carrageenan matrix, thereby reducing the free volume in the film structure.^[47] Similarly, this observation of elevated peak was also reported by Barik et al.^[66] in the study of shellac-HPMC composite. Generally, a composite film with higher T_g value is desirable due to physical stability for processing and handling qualities. The elevated temperature can also be seen at melting temperature (T_m) of Carra-HPMC composite film when it is shifted by 36.4% from 66.8°C to 105.0°C. Results show that the addition of HPMC increases the enthalpy of melting transition by 50.5% from 151.5 J/g to 306.2 J/g, which represents higher energy required to break the bond between molecules in the matrix.^[67] The hydrogen bonding interaction formed between the hydroxyl groups of carrageenan and HPMC has been discussed in NMR and FTIR analyses leads to the increment in enthalpy, and subsequently stabilized the composite film.

3.7.2 TGA analysis

TGA thermograms generally present three stages of thermal effect on the polysaccharide sample during thermal analyses.^[68] The first stage is the degradation of volatile components, such as moisture which could be perceived at temperatures of lower than 100°C for all film samples (Figure 8A). The gradual weight loss of less than 30% at this stage indicates that the films start to melt, and free water is removed when heated from ambient temperature to 100°C.^[21] The second stage is the volatilization of the plasticizers which occurs between 170°C to 225°C. This approaches to the third stage between 240°C and 275°C, which depicts the decomposition of the carrageenan polymer chain and the crosslinker as reported by Adam et al.^[19] Meanwhile,

HPMC thermogram shows only two stages of weight loss, which are around 70°C ascribed for the evaporation of loosely bound moisture and the actual decomposition of HPMC at 335.5°C with 75.3% of weight loss similar to the observation reported by Dharmalingam and Anandalakshmi.^[69]

Derivative thermogravimetry (DTG) curves are also plotted to reflect the peak at which temperature with the maximum weight loss during thermal decomposition (Figure 8B). The major decomposition stage for the control film is increased from 202.8°C to 209.5°C compared to the pure carrageenan film due to a stronger bonding between carrageenan with crosslinker and plasticizer. The inclusion of HPMC considerably delays the mass loss during the thermal decomposition, suggesting that HPMC improves the thermal stability of Carra-HPMC film. When compared to the control, the onset temperature of Carra-HPMC0.8 films is shifted to 238.9°C with a 12.3% delay. Higher degradation temperature reflects better thermal stability. This is attributed to the intermolecular interaction between carrageenan and HPMC in the matrix proven in NMR analysis which also corresponded positively to its higher mechanical properties. The summary of the degradation behaviour of different films is tabulated in Table 6 which is extracted from TGA data. Such results indicate that the existence of HPMC retards the egress of water and plasticizer from the film matrix and further supports the notion that HPMC thermally stabilizes carrageenan as the base material to some degree. This positive effect on thermal properties due to the inclusion of cellulose was also claimed in the study on the reinforcement of carrageenan film conducted by Sedayu et al.^[68]

3.8 Kinetic analysis by Broido's model

Thermal properties of different films are compared by kinetic analysis of their E_a following Broido's mathematical model. TGA has been recognized to be an effective and reliable tool to study the kinetics and to explicate the thermal stability of materials.^[70] Kinetic analysis by Broido's model allows the calculation of E_a from only one TGA curve in contrast to the other kinetic models where they use three or more TGA analyses with different heating ramps. Overall, from all DSC, TGA, and DTG curves, the major decomposition for all films occurred between 200°C to 400°C. Therefore, the E_a is calculated from one major peak at this temperature range. Figure 9 graphically presents Broido's model applied to the thermal degradation of different films.

Using logarithmic non-linear regression, all data present a good fit of Broido's model to describe the thermal degradation with high values of determination coefficient ($R^2 > 0.8997$). The changes of E_a value would occur due to the modification of polysaccharides formulation.

As in Table 7, HPMC possesses higher thermal stability since its E_a is higher with 99.2 kJ/mol compared to E_a of carrageenan (31.8 kJ/mol). It is notable that the E_a of Carra-HPMC film is lower than HPMC itself due to the presence of sulphate group of carrageenan as been examined by Jamaludin et al.^[20] The measured E_a of carrageenan is around the similar range (11.0-31.4 kJ/mol) as reported by Valenta et al.,^[71] which depends on the heating rate of TGA analysis. The E_a value of HPMC is in agreement with the value (104 kJ/mol) determined by Zaccaron et al.^[72] The E_a calculated at the major decomposition peak of Carra-HPMC0.8 thermogram is even higher up to 64.7 kJ/mol with an increment of 43.4%, confirming the positive effect of HPMC on the thermal stability of carrageenan film. The sample with the highest E_a indicates the highest resistance of its molecular structure to temperature.^[71] This effect could be linked to the good dispersion of HPMC in the carrageenan matrix and to the intermolecular interaction between carrageenan and HPMC which increases the E_a and slowed down the film decomposition due to the improved heat distribution within Carra-HPMC film. Based on the E_a values, the thermal stability of the film is in the order of HPMC>Carra-HPMC>control>carrageenan. This sequence corresponds to the previous results proven by DSC and TGA and proven the positive inclusion of HPMC as the thickening and reinforcing agent in the formulation.

In the thermal degradation process, change of enthalpy (ΔH) is the energy that reflects absorbed or released heat, where the higher values indicate low reactivity, while lower values show high reactivity.^[31] The enthalpy changes of all films reported in the table are in negative value which demonstrated an exothermic nature of reaction ($\Delta H < 0$, exothermic). These results reflect to the exothermic process indicated through the crystallization peak of the films in DSC analysis. Meanwhile, the values of the entropy change (ΔS) show that the disorder degree of films through bond dissociations are lower than the initial.^[73] The negative values indicate a quite ordered structure of the synthesized complex ($\Delta S < 0$, ordered). A lower ΔS indicates a system that is close to its thermodynamic equilibrium and less reactive.^[70] On the other hand, Gibbs energy (ΔG) represents the degree of system stability, whereby a change in state occurs spontaneously or not.^[70,73] The positive values of ΔG reveals that the thermal degradation of all films is a non-spontaneous process ($\Delta G > 0$, endergonic) and difficult to be carried out at the end of the process, subsequently increased the thermal stability of the film.^[31]

4 CONCLUSION

Introducing HPMC in the carrageenan matrix plays a vital role that significantly influenced the mechanical and thermal behaviour of the film. Carra-HPMC0.8 film

demonstrated comparable yet promising mechanical properties in terms of tensile strength, elongation at break, and capsule loop strength, confirming the positive effect of HPMC. T_g of Carra-HPMC0.8 film is improved to 65.3°C from 37.8°C of the control film. The apparent E_a of carrageenan film calculated by Broido's model is found to increase by 43.4% from 36.6 to 64.7 kJ/mol. These remarkable results prove the higher thermal stability of Carra-HPMC0.8 compared to the control without HPMC, which are attributed to the intermolecular interactions between carrageenan and HPMC, being supported by ^1H NMR and FTIR analyses. Plant-based materials introduced in this study, which are carrageenan and HPMC offer a better commercial prospect to a wider consumers preference. This distinct advantage over gelatin is a key driver for the development of Carra-HPMC hard capsule on a larger scale. The processing steps of preparing hard capsules from carrageenan and HPMC need to be improved and modifications should be done to ensure the establishment of hard capsules with higher-level quality and to be comparable to gelatin.

ACKNOWLEDGEMENTS

The authors would like to thank the Ministry of Higher Education for providing financial support under Fundamental Research Grant Scheme (FRGS) No. FRGS/1/2019/TK05/UMP/02/2 (University reference RDU1901111) and Universiti Malaysia Pahang for laboratory facilities as well as additional financial support under Internal Research grant PGRS2003131.

NOMENCLATURE

Symbols

E_a	activation energy (kJ/mol)
w_t	weight at any time (g)
w_o	initial weight (g)
w_∞	weight of residue (g)
R	universal gas constant ($\text{mol}^{-1} \text{K}^{-1}$)
T	temperature (K)
A	pre-exponential factor (min^{-1})
T_g	glass transition temperature ($^{\circ}\text{C}$)
T_m	melting temperature ($^{\circ}\text{C}$)
T_c	crystallization temperature ($^{\circ}\text{C}$)
ΔH_m	melting enthalpy (J/g)

ΔH_c	crystallization enthalpy (J/g)
ΔS	entropy (J/K·mol)
ΔH	enthalpy (kJ/mol)
ΔG	Gibbs free energy (kJ/mol)

Dimensionless numbers

y	degree of conversion
R ²	coefficient of determination

REFERENCES

- [1] L. L. Augsburger, S. W. Hoag, *Pharm. Dos. Forms* **2017**, 1.
- [2] S. B. Majee, D. Avlani, G. R. Biswas, *Int. J. Pharm. Pharm. Sci.* **2017**, 9, 1.
- [3] N. Hassan, T. Ahmad, N. M. Zain, *J. Food Sci.* **2018**, 83, 2903.
- [4] Z. Sabara, A. Mutmainnah, U. Kalsum, I. N. Afiah, I. Husna, A. Saregar, Irzaman, R. Umam, *Int. J. Biomater.* **2022**, 2022, 9889127.
- [5] M. A. Hamdan, K. N. M. Amin, R. Jose, D. Martin, F. Adam, *Food Hydrocoll. Heal.* **2021**, 100023.
- [6] F. Song, B. Zhang, X. Ge, Y. Jiang, *Int. J. Biol. Macromol.* **2021**, 189, 715.
- [7] S. Y. Ock, W. S. Lim, G. D. Park, M. H. Lee, H. J. Park, *Polym. Test.* **2020**, 91, 106871.
- [8] N. Zhang, X. Li, J. Ye, Y. Yang, Y. Huang, X. Zhang, M. Xiao, *Polymers* **2020**, 12, 1.
- [9] M. A. R. D. Fauzi, P. Pudjiastuti, E. Hendradi, R. T. Widodo, M. C. I. M. Amin, *Int. J. Polym. Sci.* **2020**, 2020, 3565931.
- [10] F. Adam, M. A. Hamdan, S. H. Abu Bakar, in *Industrial Applications of Biopolymers and their Environmental Impact* (Eds: A. A. Maamun, J. Y. Chen), CRC Press, Boca Raton, Florida **2020**, Ch. 9.
- [11] Z. M. Al-Nahdi, A. Al-Alawi, I. Al-Marhobi, *J. Mar. Biol.* **2019**, 2019, 5183261.
- [12] M. Yadav, F. Chiu, *Carbohydr. Polym.* **2019**, 211, 181.
- [13] F. Adam, J. Jamaludin, S. H. Abu Bakar, R. Abdul Rasid, Z. Hassan, *Cogent Eng.* **2020**, 7.
- [14] H. P. S. A. Khalil, Y. Y. Tye, C. K. Saurabh, C. P. Leh, T. K. Lai, E. W. N. Chong, M. R. N. Fazita, J. M. Hafidz, A. Banerjee, M. I. Syakir, *Express Polym. Lett.* **2017**, 11, 244.
- [15] D. R. Bagal-Kestwal, M. H. Pan, B.H. Chiang, *Bio Monomers Green Polym. Compos. Mater.* **2019**, 117.
- [16] G. Sun, T. Liang, W. Tan, L. Wang, *Food Hydrocoll.* **2018**, 85, 61.
- [17] M. A. Hamdan, F. Adam, K. N. Mohd Amin, *Int. J. Innov. Sci. Technol.* **2018**, 3, 457.
- [18] M. A. Hamdan, N. A. Ramli, N. A. Othman, K. N. Mohd Amin, F. Adam, in *Mater. Today Proc.* (Eds: R. Abdul Rasid, H. D. Setiabudi), Elsevier Ltd, United Kingdom **2021**, 56.
- [19] F. Adam, M. A. Hamdan, S. Hana, A. Bakar, M. Yusoff, R. Jose, *Chem. Eng. Commun.* **2020**, 208, 741.
- [20] J. Jamaludin, F. Adam, R. A. Rasid, Z. Hassan, *Chem. Eng. Res. Bull.* **2017**, 19, 80.
- [21] S. K. Owusu-Ware, J. S. Boateng, B. Z. Chowdhry, M. D. Antonijevic, *Int. J. Pharm. X* **2019**, 1, 100033.
- [22] E. Faulhammer, A. Kovalcik, V. Wahl, D. Markl, F. Stelzer, S. Lawrence, J. G. Khinast, A. Paudel, *Int. J. Pharm.* **2016**, 511, 840.
- [23] X. Liu, Z. Ji, W. Peng, M. Chen, L. Yu, F. Zhu, *Food Hydrocoll.* **2020**, 104, 105734.

- [24] N. N. Nyamweya, *Futur. J. Pharm. Sci.* **2021**, 7, 18.
- [25] L. Tian, H. Fan, H. Liu, Z. Tong, T. Liu, Y. Zhang, *J. Appl. Polym. Sci.* **2021**, 138, 1.
- [26] S. Velpula, S. R. Beedu, K. Rupula, *J. Mater. Sci. Mater. Electron.* **2022**, 33, 2677.
- [27] H. Homayouni, G. Kavooosi, S. M. Nassiri, *LWT - Food Sci. Technol.* **2017**, 77, 503.
- [28] J. Wang, M. Caceres, S. Li, A. Deratani, *Macromol. Chem. Phys.* **2017**, 218, 1.
- [29] A. Adhikari, J. E. Polli, *Pharm. Res.* **2020**, 37, 4.
- [30] N. A. Othman, F. Adam, N. H. Mat Yasin, in *Mater. Today Proc.* (Eds: W. A. Wan Azmi, J. Mahmud, M. Rahman), Elsevier Ltd, United Kingdom **2020**, 77.
- [31] M. Khalil, F. Z. Alqahtany, *J. Inorg. Organomet. Polym. Mater.* **2020**, 30, 3750.
- [32] R. R. R. Cecci, A. A. Passos, N. R. V. Albino, D. S. Vicente, A. S. S. Duarte, M. I. B. Tavares, *J. Mater. Sci. Eng. B* **2020**, 10.
- [33] A. L. Ellis, T. B. Mills, I. T. Norton, A. B. Norton-Welch, *J. Colloid Interface Sci.* **2019**, 538, 165.
- [34] M. Nemazifard, G. Kavooosi, Z. Marzban, N. Ezedi, *Int. J. Food Prop.* **2017**, 20, 1501.
- [35] N. A. Ramli, N. Ali, S. Hamzah, N. I. Yatim, *Heliyon* **2021**, 7, e06649.
- [36] L. Youssouf, L. Lallemand, P. Giraud, F. Soulé, A. Bhaw-Luximon, O. Meilhac, C. L. D'Hellencourt, D. Jhurry, J. Couprie, *Carbohydr. Polym.* **2017**, 166, 55.
- [37] M. H. Abu Bakar, N. H. Azeman, N. N. Mobarak, M. H. H. Mokhtar, A. A. A. Bakar, *Polymers* **2020**, 12, 1.
- [38] N. G. Voron'ko, S. R. Derkach, M. A. Vovk, P. M. Tolstoy, *Carbohydr. Polym.* **2017**, 169, 117.
- [39] A. Lu, E. Petit, K. Jelonek, A. Orchel, J. Kasperczyk, Y. Wang, F. Su, S. Li, *Int. J. Biol. Macromol.* **2020**, 154, 39.
- [40] M. Amin, M. A. Hussain, S. Aqsa, B. Bukhari, M. Sher, Z. Shafiq, *Cellul. Chem. Technol.* **2017**, 51, 245.
- [41] P. L. Nasatto, F. Pignon, J. L. M. Silveira, M. E. R. Duarte, M. D. Nosedá, M. Rinaudo, *Polym.* **2015**, 7, 777.
- [42] A. M. Ili Balqis, M. A. R. Nor Khaizura, A. R. Russly, Z. A. Nur Hanani, *Int. J. Biol. Macromol.* **2017**, 103, 721.
- [43] R. B. Bodini, J. das G. L. Guimarães, C. A. Monaco-Lourenço, R. Aparecida de Carvalho, *J. Drug Deliv. Sci. Technol.* **2019**, 51, 403.
- [44] E. M. Pacheco-Quito, R. Ruiz-Caro, J. Rubio, A. Tamayo, M. D. Veiga, *Mar. Drugs* **2020**, 18.
- [45] J. Suksaeree, N. Nawathong, R. Anakkawee, W. Pichayakorn, *AAPS PharmSciTech* **2017**, 18, 2427.
- [46] W. Chi, L. Cao, G. Sun, F. Meng, C. Zhang, J. Li, *J. Clean. Prod.* **2020**, 244, 118862.
- [47] A. Aydogdu, G. Sumnu, S. Sahin, *Carbohydr. Polym.* **2018**, 181, 234.
- [48] C. M. Oh, P. Wan, S. Heng, L. W. Chan, *AAPS PharmSciTech* **2015**, 16, 466.
- [49] P. Hiremath, K. Nuguru, V. Agrahari, in *Handbook of Pharmaceutical Wet Granulation* (Eds: A. S. Narang, S. I. F. Badawy), Academic Press, Massachusetts, United States **2019**, Ch. 8.
- [50] H. Abral, A. Basri, F. Muhammad, Y. Fernando, F. Hafizulhaq, M. Mahardika, E. Sugiarti, S. M. Sapuan, R. A. Ilyas, I. Stephane, *Food Hydrocoll.* **2019**, 93, 276.
- [51] H. Kargazadeh, M. Mariano, J. Huang, N. Lin, I. Ahmad, A. Dufresne, S. Thomas, *Polymer* **2017**, 132, 368.
- [52] D. I. Munthoub, W. A. W. A. Rahman, *Sains Malaysiana* **2011**, 40, 713.
- [53] M. J. Dille, I. J. Haug, K. I. Draget, in *Handbook of Hydrocolloids* (Eds: O. P. Glyn, A. W. Peter), Elsevier, Amsterdam, The Netherlands **2021**, Ch. 34.
- [54] M. H. Fakharian, N. Tamimi, H. Abbaspour, A. Mohammadi Nafchi, A. A. Karim, *Carbohydr. Polym.* **2015**, 132, 156.

- [55] M. A. Hamdan, N. H. Sulaiman, K. N. Mohd Amin, F. Adam, in *IOP Conf. Series: Materials Science and Engineering* (Eds: Z. Ismail, A. C. Benedict, N. Ahmad), IOP Publishing, United Kingdom **2021**, 1092, 012057
- [56] A. M. Smith, L. Grover, Y. Perrie, *J. Pharm. Pharmacol.* **2010**, 62.
- [57] N. H. Zainal Abedin, A. H. Abu Bakar, *Int. J. Biol. Macromol.* **2018**, 114, 710.
- [58] A. Jones, M. Zeller, S. Sharma, *Prog. Biomater.* **2013**, 2, 12.
- [59] M. Fu, J. Blechar, A. Sauer, J. Al-Gousous, P. Langguth, *Pharmaceutics* **2020**, 12, 1.
- [60] N. Glube, L. Von Moos, G. Duchateau, *Results Pharma Sci.* **2013**, 3, 1.
- [61] L. Sánchez-González, M. Vargas, C. González-Martínez, A. Chiralt, M. Cháfer, *Food Hydrocoll.* **2009**, 23, 2102.
- [62] M. Shojaei, M. Eshaghi, L. Nateghi, *J. Food Process. Preserv.* **2019**, 43, 1.
- [63] J. Liu, H. Wang, P. Wang, M. Guo, S. Jiang, X. Li, S. Jiang, *Food Hydrocoll.* **2018**, 83, 134.
- [64] J. W. Y. Liew, K. S. Loh, A. Ahmad, K. L. Lim, W. R. Wan Daud, *PLoS One* **2017**, 12, 1.
- [65] M. H. Shoaib, R. I. Yousuf, F. R. Ahmed, F. R. Ali, F. Qazi, K. Ahmed, F. Zafar, in *Polymer Coatings: Technology and Applications* (Eds: Inamuddin, R. Boddula, M. I. Ahamed, A. M. Asiri), Scrivener Publishing LLC, Massachusetts, United States **2020**, Ch. 12.
- [66] A. Barik, T. Patnaik, P. Parhi, S. K. Swain, R. K. Dey, *Polym. Bull.* **2017**, 74, 3467.
- [67] S. C. Joshi, *Materials* **2011**, 4, 1861.
- [68] B. B. Sedayu, M. J. Cran, *Polymers* **2020**, 12, 1145.
- [69] K. Dharmalingam, R. Anandalakshmi, *Int. J. Biol. Macromol.* **2019**, 134, 815.
- [70] G. Ozsin, *BSEU J. Sci.* **2020**, 7, 313.
- [71] T. Valenta, B. Lapčiková, L. Lapčík, *Colloids Surfaces A Physicochem. Eng. Asp.* **2018**, 555, 270.
- [72] M. Zaccaron, R. V. B. Oliveira, M. Guiotoku, A. T. N. Pires, V. Soldi, *Polym. Degrad. Stab.* **2005**, 90, 21.
- [73] D. Çanakçı, *Sci. Rep.* **2020**, 10.

Figure Captions

FIGURE 1 (A) Zeta potential for each material in composite and (B) the effect of HPMC concentration on the zeta potential of composite

Abbreviations: HPMC, hydroxypropylmethyl cellulose; alg, alginic acid; PEG, polyethylene glycol.

FIGURE 2 (A) ^1H NMR spectrum of carrageenan

FIGURE 2 (B) ^1H NMR spectrum of HPMC

FIGURE 2 (C) ^1H NMR spectrum of Carra-HPMC composite

FIGURE 3 Schematic representation of the proposed hydrogen bonding interaction between carrageenan and HPMC

FIGURE 4 FTIR spectra of (A) carrageenan, HPMC, and Carra-HPMC and (B) film at different HPMC concentrations

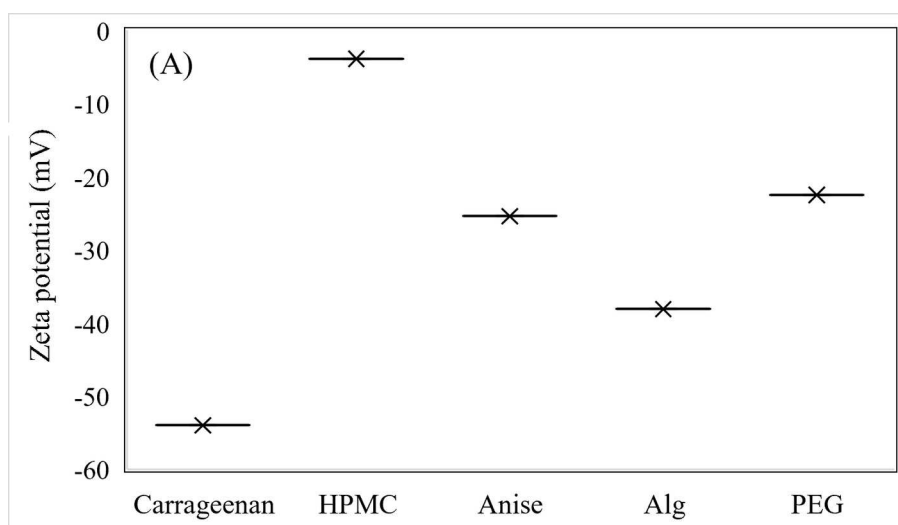
FIGURE 5 Effect of HPMC concentration on the (A) viscosity and tensile strength, and (B) elongation at break of film and hard capsule loop strength

FIGURE 6 Images of films and hard capsules, and their surface morphology at different HPMC concentrations

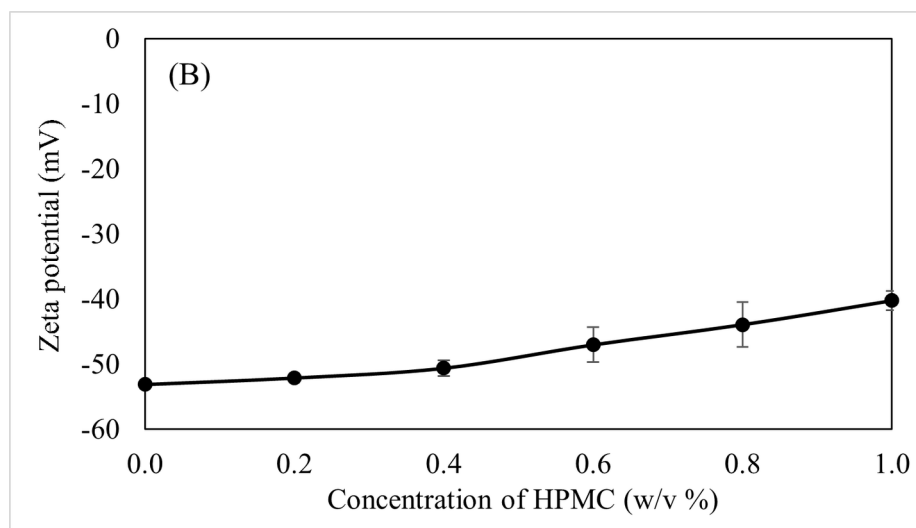
FIGURE 7 DSC thermograms of carrageenan, HPMC, and films at different HPMC concentrations

FIGURE 8 TGA (A) and DTG (B) thermograms of carrageenan, HPMC and films at different HPMC concentrations

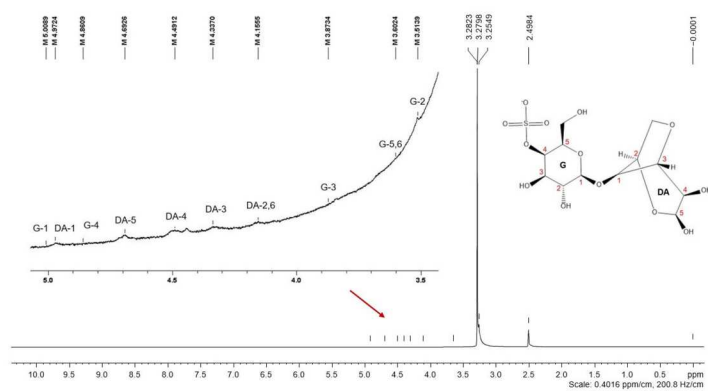
FIGURE 9 Graphical representation of Broido's plots for degradation of (A) carrageenan, (B) HPMC, and (C) films at different HPMC concentrations



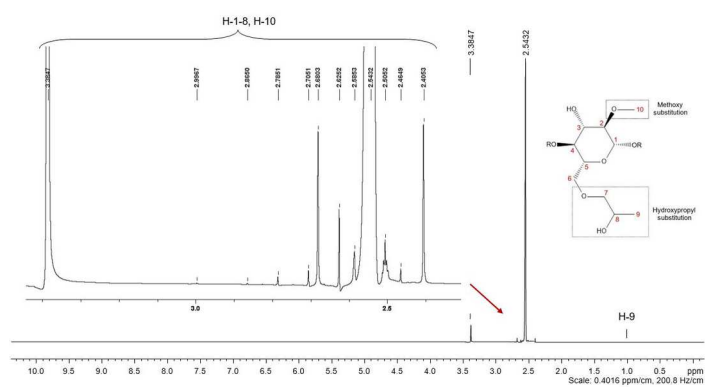
CJCE_24595_CJCE-21-0682.R1_Figure 1A.tif



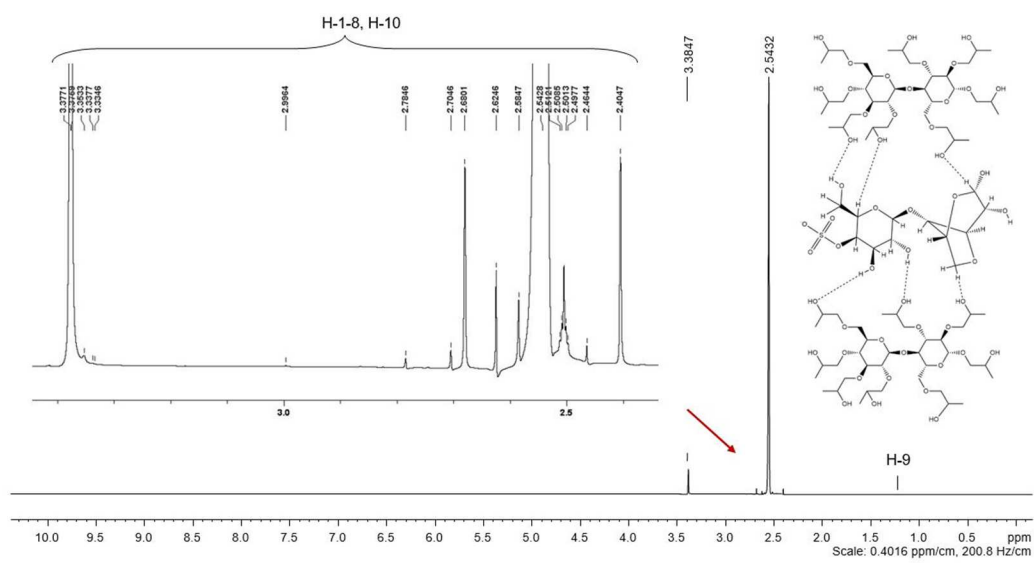
CJCE_24595_CJCE-21-0682.R1_Figure 1B.tif



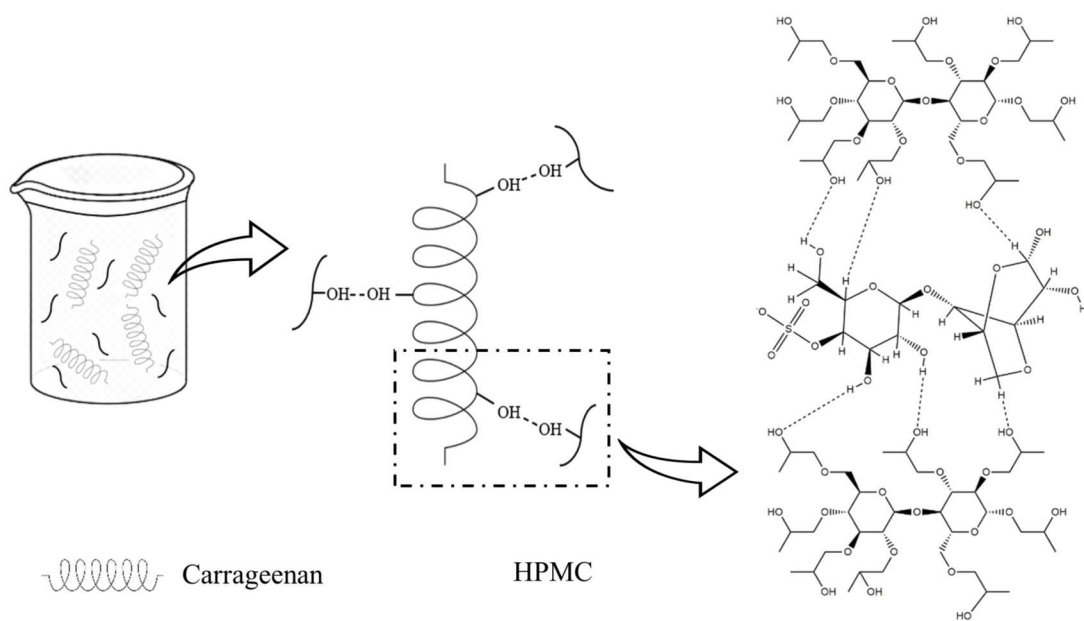
CJCE_24595_Figure_2(A).tiff



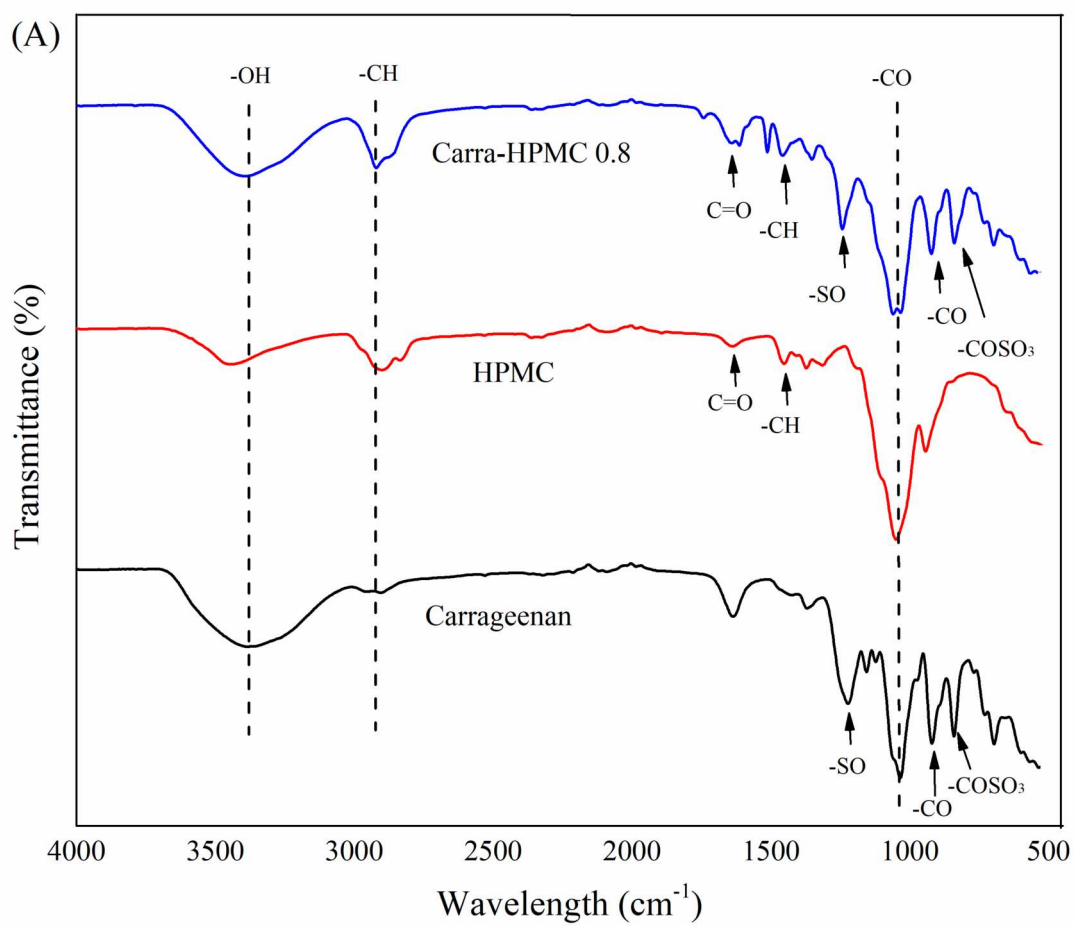
CJCE_24595_CJCE-21-0682.R1_Figure 2B.tif



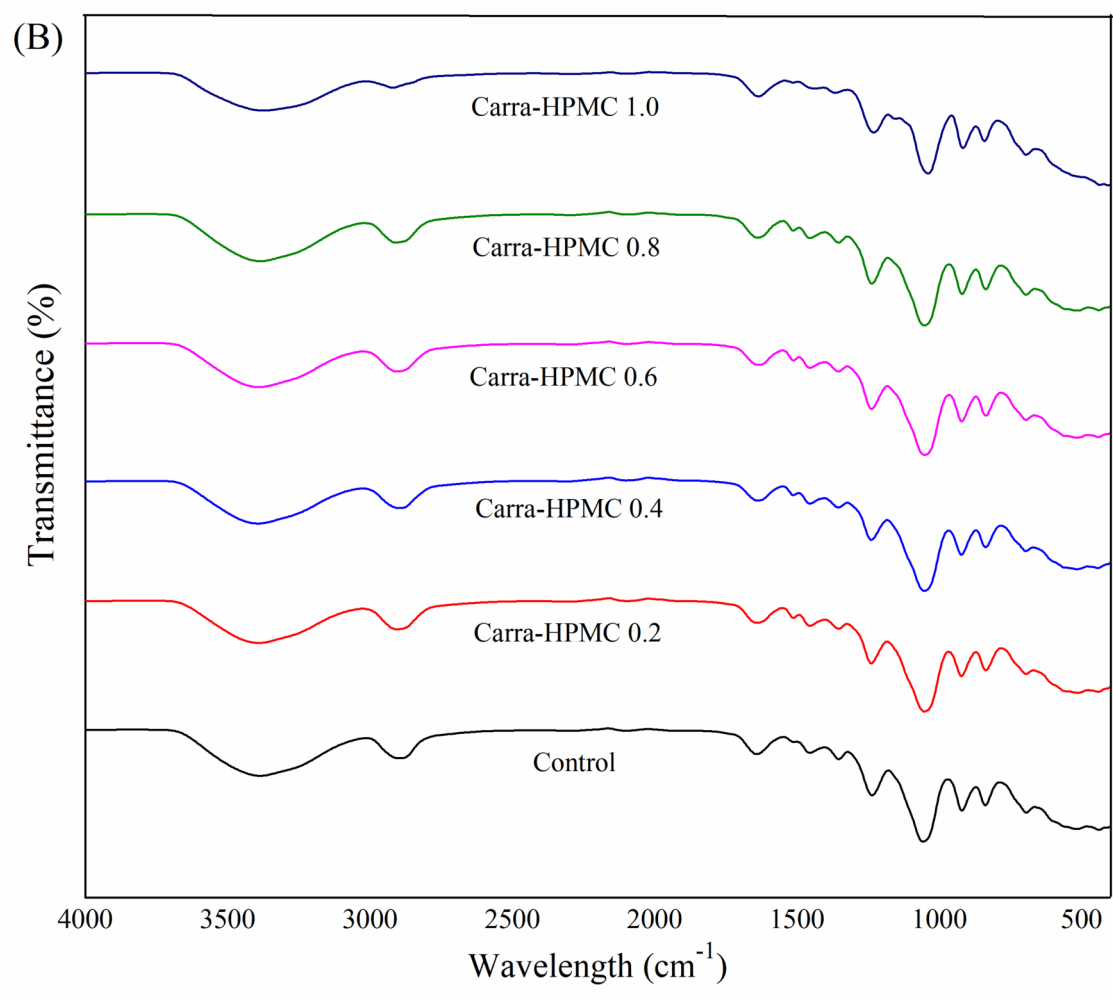
CJCE_24595_Figure_2(C).tif



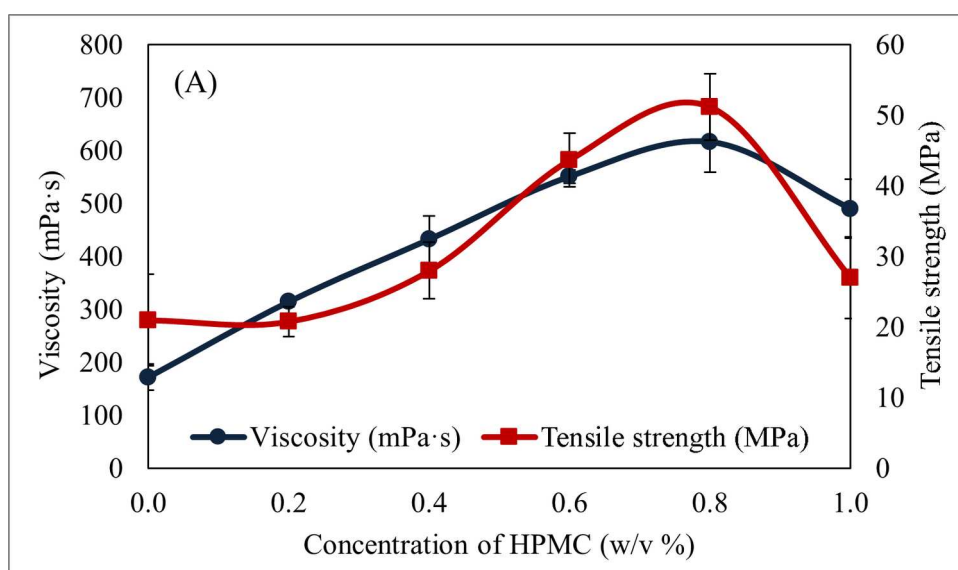
CJCE_24595_Figure_3.tif



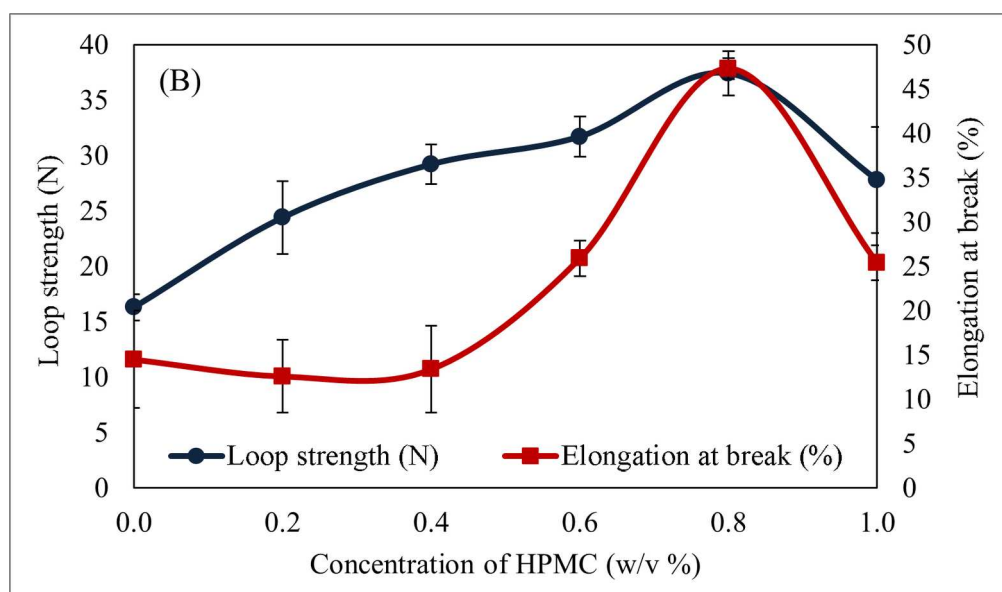
CJCE_24595_Figure_4(A).tif



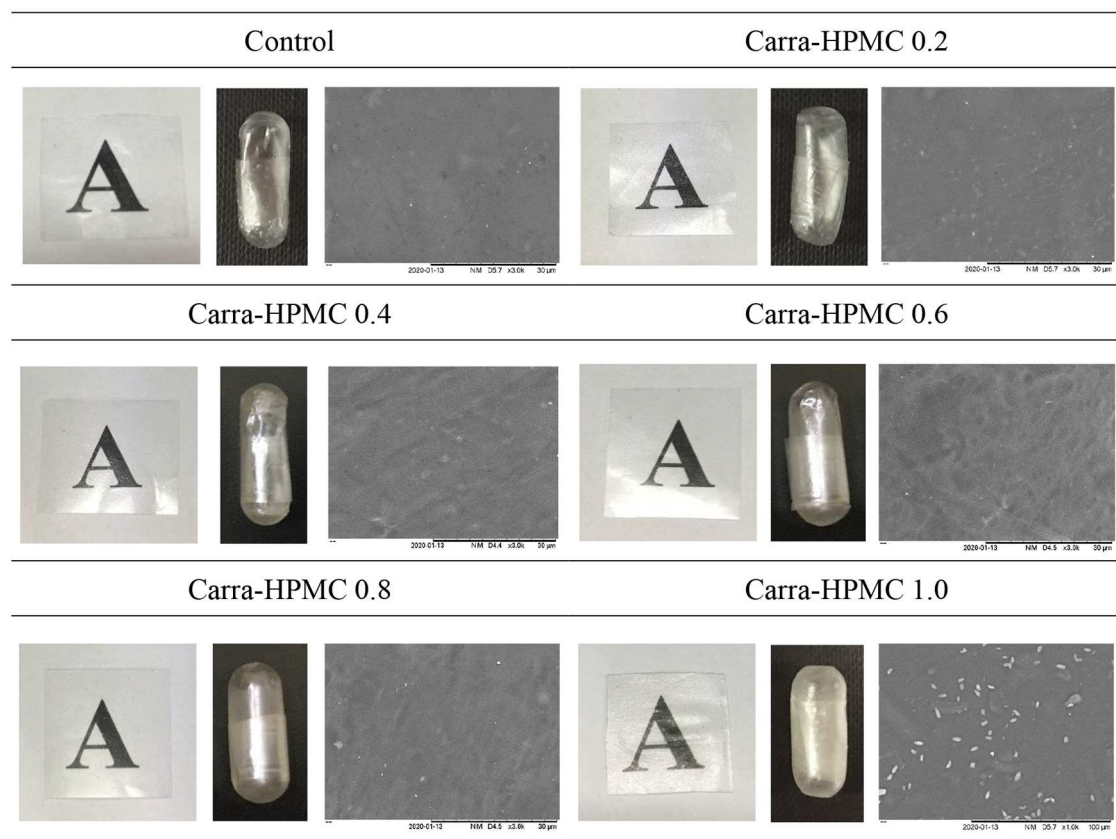
CJCE_24595_Figure_4(B).tif



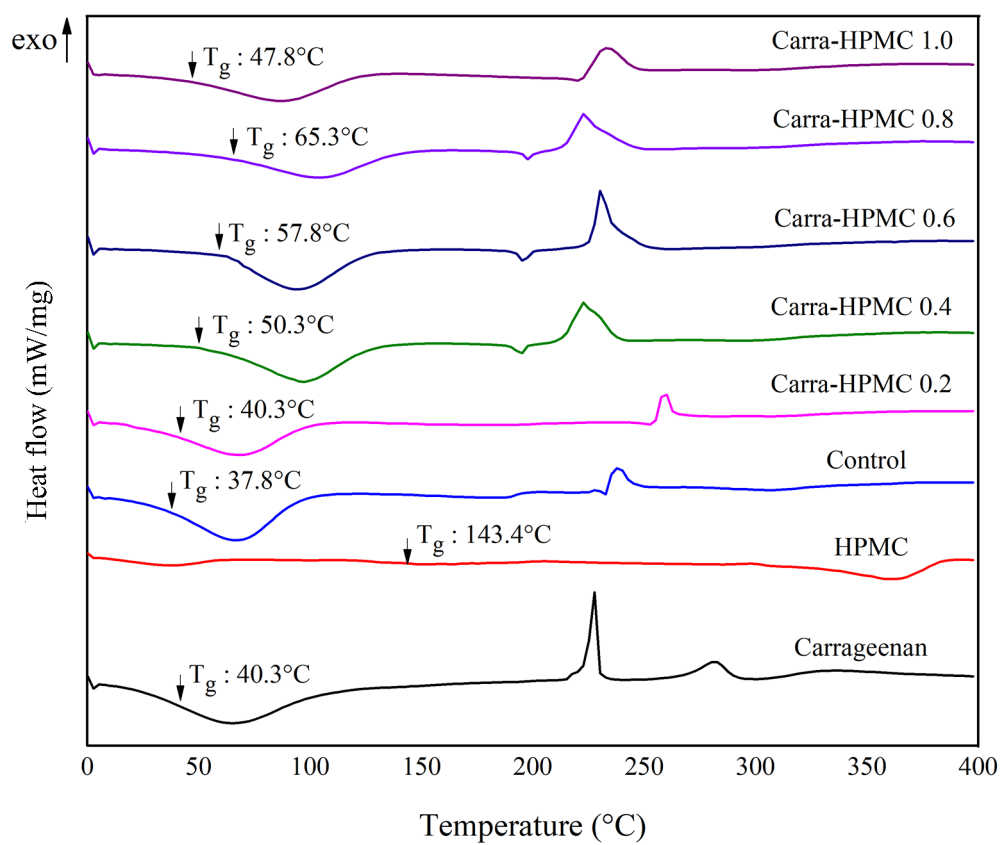
CJCE_24595_CJCE-21-0682.R1_Figure 5A.tif



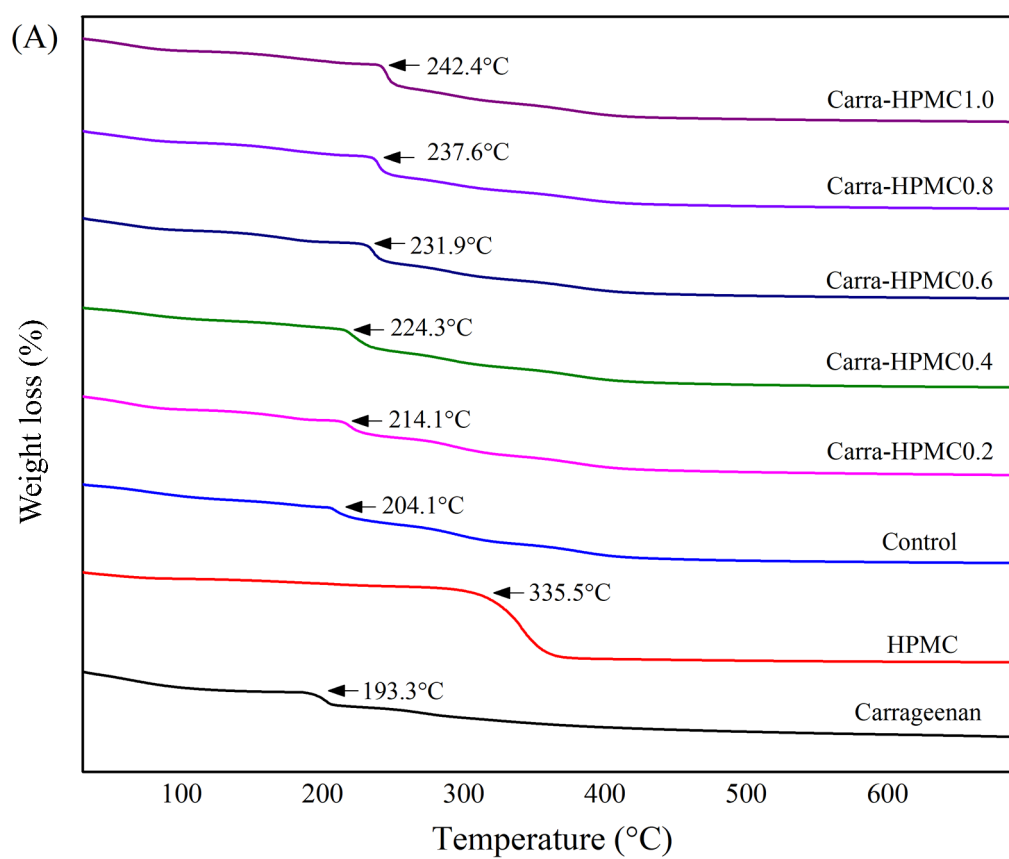
CJCE_24595_CJCE-21-0682.R1_Figure 5B.tif



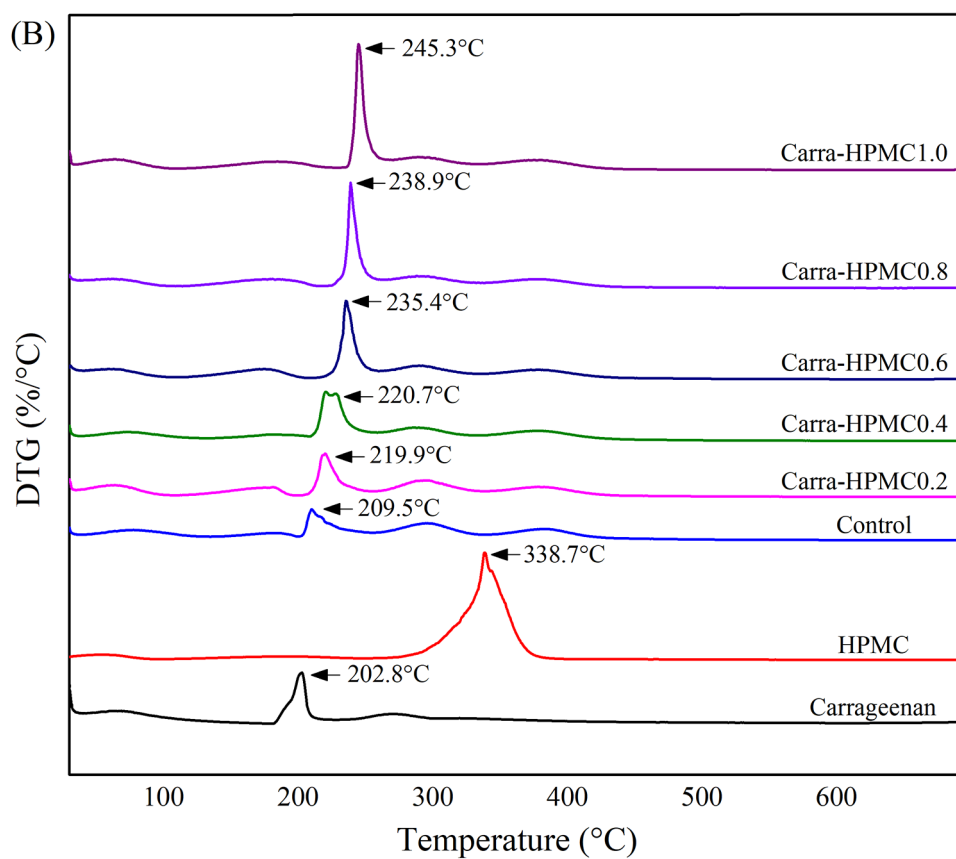
CJCE_24595_CJCE-21-0682.R1_Figure 6.tif



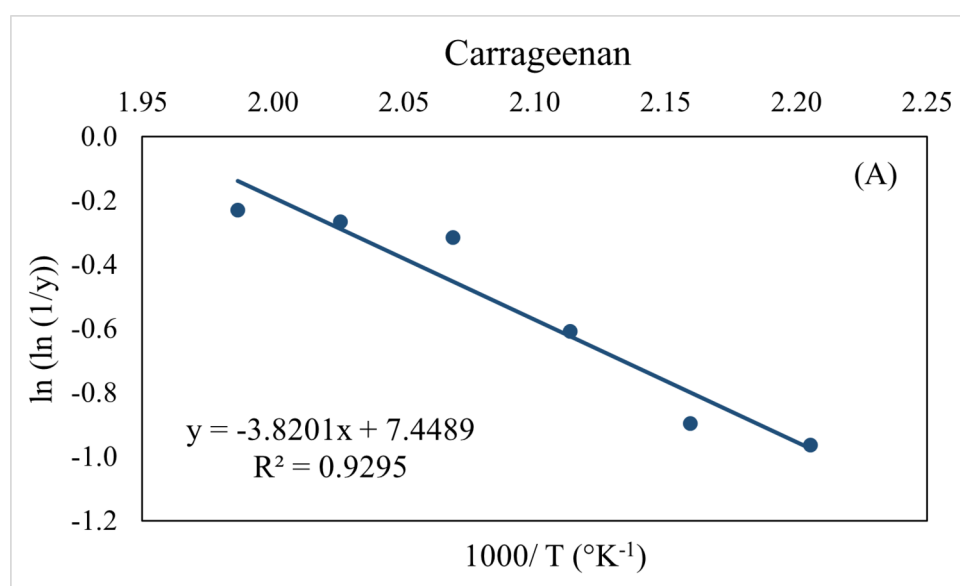
CJCE_24595_CJCE-21-0682.R1_Figure 7.tif



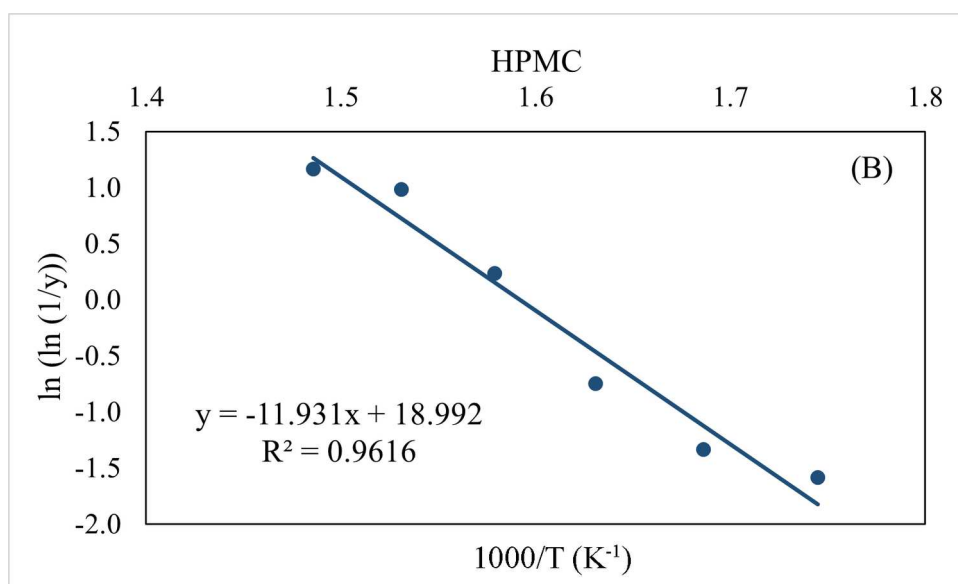
CJCE_24595_CJCE-21-0682.R1_Figure 8A.tif



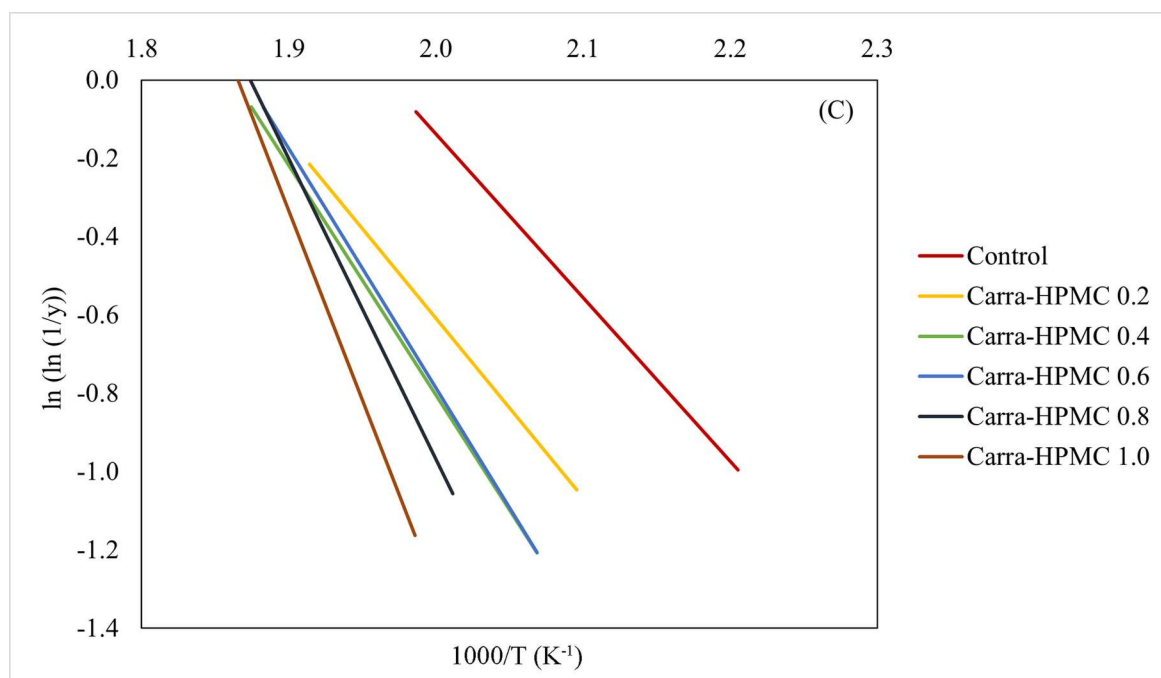
CJCE_24595_CJCE-21-0682.R1_Figure 8B.tif



CJCE_24595_Figure_9(A).tif



CJCE_24595_CJCE-21-0682.R1_Figure 9B.tif



CJCE_24595_CJCE-21-0682.R1_Figure 9C.tif

Table Captions

TABLE 1 Formulation of Carra-HPMC composite films and hard capsules

Samples	Carrageenan (w/v%)	HPMC (w/v%)
Control	2.0	0
Carra-HPMC 0.2	2.0	0.2
Carra-HPMC 0.4	2.0	0.4
Carra-HPMC 0.6	2.0	0.6
Carra-HPMC 0.8	2.0	0.8
Carra-HPMC 1.0	2.0	1.0

TABLE 2 ¹H NMR results of composite in comparison with carrageenan and HPMC

Samples	Integration of peak at 3.2-3.4 ppm	Number of protons at 2.35-2.99 ppm	Integration of peak at 1.0-1.3 ppm
Carrageenan	3.255, 3.279, 3.282	0.128	No peak detected
HPMC	3.385	23.572	1.020
Carra-HPMC	3.335, 3.338, 3.353, 3.376, 3.377, 3.385	25.617	1.232

TABLE 3 Comparison on the properties of Carra-HPMC hard capsule in current work and commercial gelatin hard capsule

Hard Capsules	Viscosity (mPa·s)	Loop Strength (N)	T_m (°C)	Moisture Content (%)	Disintegration Time (min)
Carra-HPMC	616	37.4	105.0	14.6	18.7
Gelatin	750-1000 ^{[53][54]}	115.0 ^[17]	187.3 ^[55]	13.0 ^[56]	15.0 ^[9]

Abbreviations: T_m, melting temperature.

TABLE 4 Effect of HPMC concentration on the moisture content of film and disintegration time of hard capsule

Samples	Moisture content (%)	Disintegration time (min)
Control	23.2 ± 2.8	10.6 ± 2.1
Carra-HPMC 0.2	21.4 ± 2.1	12.8 ± 1.0
Carra-HPMC 0.4	16.0 ± 2.4	14.7 ± 1.7
Carra-HPMC 0.6	17.1 ± 3.0	17.1 ± 1.6
Carra-HPMC 0.8	14.6 ± 1.2	18.7 ± 1.8
Carra-HPMC 1.0	12.9 ± 1.9	23.6 ± 2.2

TABLE 5 Transition temperatures and enthalpies of carrageenan, HPMC, and films at different HPMC concentrations

Samples	T_g (°C)	T_m (°C)	ΔH_m (J/g)	T_c (°C)	ΔH_c (J/g)
Carrageenan	40.3	65.3	229.8	227.8	71.6
HPMC	143.4	358.8	179.3	-	-
Control	37.8	66.8	151.5	238.0	79.8
Carra-HPMC 0.2	40.3	74.1	189.2	258.7	49.2
Carra-HPMC 0.4	50.3	96.5	238.8	222.0	152.5
Carra-HPMC 0.6	57.8	95.4	323.7	231.3	183.7
Carra-HPMC 0.8	65.3	105.0	306.2	222.7	137.1
Carra-HPMC 1.0	47.8	86.9	191.5	232.6	72.85

Abbreviations: T_g, glass transition; T_m, melting temperature; ΔH_m, melting enthalpy, T_c, crystallization temperature; ΔH_c, crystallization enthalpy.

TABLE 6 Thermal degradation behaviour of films by TGA analysis

Samples	Step	Temperature range (°C)	Weight loss at step end (%)	Temperature at	
				maximum degradation rate (°C)	Residues at 700°C (%)
Carrageenan	1	30-200	26.7	202.8	34.3
	2	200-700	39.0		
HPMC	1	30-200	11.0	353.4	9.6
	2	200-700	79.4		
Control	1	30-200	23.2	209.5	21.6
	2	200-700	55.3		
Carra-HPMC 0.2	1	30-200	23.8	219.9	21.6
	2	200-700	54.0		
Carra-HPMC 0.4	1	30-200	20.4	220.7	20.7
	2	200-700	58.9		
Carra-HPMC 0.6	1	30-200	24.1	235.4	19.9
	2	200-700	56.0		
Carra-HPMC 0.8	1	30-200	23.1	238.9	22.5
	2	200-700	54.4		
Carra-HPMC 1.0	1	30-200	22.9	245.3	17.2
	2	200-700	59.9		

TABLE 7 Kinetic and thermodynamic parameters of thermal degradation by Broido's model.

Samples	E_a (kJ/mol)	A	R²	ΔS (J/K·mol)	ΔH (kJ/mol)	ΔG (kJ/mol)
Carrageenan	31.8	1.7×10^3	0.9295	-186.9	-3925.3	8.5×10^4
HPMC	99.2	1.8×10^8	0.9565	-93.2	-5109.9	5.3×10^4
Control	36.6	2.7×10^3	0.8997	-183.3	-3976.1	8.5×10^4
Carra-HPMC 0.2	37.7	4.7×10^3	0.9565	-178.7	-4061.5	8.4×10^4
Carra-HPMC 0.4	43.7	1.7×10^4	0.9103	-168.1	-4062.2	7.9×10^4
Carra-HPMC 0.6	54.9	2.5×10^5	0.9504	-146.1	-4173.2	7.0×10^4
Carra-HPMC 0.8	64.7	2.2×10^6	0.9504	-127.9	-4192.5	6.1×10^4
Carra-HPMC 1.0	85.8	2.5×10^8	0.9416	-88.7	-4224.6	4.2×10^4

Abbreviations: E_a, activation energy; A, pre-exponential factor; R², coefficient of determination; ΔS, entropy; ΔH, enthalpy; ΔG, Gibbs free energy.